ISSN (Print) 1226-1750
ISSN (Online) 2233-6656
Journal of Magnetics 27(1), 65-71 (2022) https://doi.org/10.4283/JMAG.2022.27.1.065

Experiment Study and Machine Learning Prediction of Damping Performance of Ferrofluid Dynamic Vibration Absorber

Xiao Liu and Decai Li*

State Key Laboratory of Tribology, Tsinghua University, Beijing 100084, China

(Received 8 August 2021, Received in final form 17 March 2022, Accepted 18 March 2022)

In this research, we study four influence factors of the damping performance of ferrofluid dynamic vibration absorber, as well as predict and optimize the damping performance by machine learning method. The vibration absorber in our research is based on the second order buoyancy principle, which consists of a non-magnetic container, a small amount of ferrofluid and a permanent magnet. The effects of the initial amplitude, the cone angle of the cover, the thickness of the gasket and the mass of the ferrofluid on the damping performance are investigated by experiments. Based on the experiment data, we use BP neural network to establish a prediction model between the four influence factors and the damping performance. The prediction error of damping efficiency predicted by BP neural network is mainly within ± 0.4%. Meanwhile, the determination coefficient R^2 of test data is 0.96242. The both indicate that BP neural network has a good performance in predicting the damping efficiency. Furthermore, we use the search algorithm to find the optimized values of each influence factor through the prediction model and the high damping efficiency is confirmed by experiments. Our work introduces machine learning into the field of vibration absorber designing, which provides an innovative method for the rapid design of high efficiency vibration absorber.

Keywords : ferrofluid, dynamic vibration absorber, machine learning, damping performance, neural network

1. Introduction

Vibration absorption is essential for various kinds of industrial applications [1]. Ferrofluid is a stable colloid composed of carrier fluid and magnetic nanoparticles dispersed by the surfactant, which has excellent magnetic and rheological properties under an external magnetic field [2-5]. Ferrofluid dynamic vibration absorber has the advantages of more simple structure, longer life and less energy consuming compared to conventional vibration absorber [6-10]. Therefore, ferrofluid dynamic vibration absorber can be used in spacecraft where the energy is scarce. National Aeronautics and Space Administration (NASA) first developed a ferrofluid dynamic vibration absorber for Radio Astronomical Exploration satellite in 1966, which can effectively suppress the vibration caused by the stable system of the satellite [11]. After that, some scholars have developed several types of dynamic vibration absorber utilizing ferrofluid. Most of the ferrofluid vibration absorbers are developed based on the second order buoyancy principle (ferrofluid can suspend the immersed permanent magnet) of ferrofluid [7, 12-15]. No external power supply is one of the most important advantages for these vibration absorbers. Yang *et al.* proposed a ferrofluid vibration absorber which had an excellent performance of small amplitude (less than 1 mm) and small frequency (less than 1 Hz). This vibration absorber is suitable for solving the vibration problems in spacecraft technology especially [15]. Damping performance is the most important property of the vibration absorber. Yao *et al*. predicted the damping performance of the absorber according to the measured damping coefficient. However, they need to obtain the physical parameters, boundary conditions and initial conditions of the material, and also needs to solve complex control equations. Meanwhile, the deviation between the experimental value and the theoretical value is relatively large in some cases [16]. Until now, there is no feasible method to predict the damping efficiency of ferrofluid dynamic vibration absorber.

In this study, we propose a ferrofluid dynamic vibration absorber based on the second order buoyancy principle of ferrofluid, that is, the ferrofluid can suspend permanent

*Corresponding author: Tel: +8610 6279253
Fax: +8610 6279253, e-mail: lidecai@mail.tsinghua.edu.cn

magnet. The vibration absorber has the characteristics of simple structure and passive vibration reduction. Thus, it can be used in spacecraft technology. The influence of the initial amplitude, the cone angle of the cover, the thickness of the gasket and the mass of the ferrofluid on the damping performance of the vibration absorber is studied experimentally. The initial amplitude is investigated to estimate the amplitude at which the shock absorber is most suitable to work. The cone angle of the cover determines the restoring force of the ferrofluid, which is strongly correlated with the damping efficiency. The thickness of the gasket determined the friction force between the ferrofluid and the shell. If the thickness of the gasket is too small, the friction force will be too large and the motion of permanent magnet and ferrofluid is restricted, thus the vibration energy cannot be dissipated through the motion. If the thickness of the gasket is too large, the friction force will be too small to dissipate the vibration energy. The mass of ferrofluid also determines the friction force, and neither too large nor too little ferrofluid can provide appropriate friction force. The results show that the initial amplitude has little influence on the damping efficiency; the damping efficiency increases first and then decreases with the increase of the mass of ferrofluid and the gasket thickness; the appropriate cone angle of the gasket can improve the damping efficiency of the shock absorber. We have predicted the damping performance by machine learning. An influence factors-damping performance prediction model is obtained by using BP neural network. We find that the mean squared error (MSE) of BP neural network is the smallest when the number of neurons in the hidden layer is 7. In this case, the error between predicted value and real value of the damping efficiency is mainly distributed within ± 0.4%, and the determination coefficient R^2 of test data is 0.96242, which all indicate that BP neural network has a good performance in predicting damping efficiency. Then, we use search algorithm to optimize the values of the influence factors. The best damping efficiency 94.03 % is obtained when the amplitude is 1 mm, the cone angle of the cover is 15°, the thickness of the gasket is 5.2 mm and the mass of the ferrofluid 36.9 g. It is close to the experimental value under the same parameters. Our results indicate that machine learning could be a powerful tool in designing the structure parameters of ferrofluid dynamic vibration absorber.

2. Methods and Experiments

2.1. Structure design

The scheme of ferrofluid dynamic vibration absorber is shown in Fig. 1. It includes a container made of non-magnetic materials, a cover with cone angle, a gasket and a permanent magnet coated with ferrofluid. The cone angle of the cover can provide restoring force to the permanent magnet, which can ensure that the permanent magnet is in the center of the vibration absorber. The shell is made of lightweight, non-magnetic aluminum alloy. The cover is made of acrylic material, which is easy to manufacture the cone angle. The permanent magnet is made of NdFeB, which possesses the characteristic of high magnetic performance, good mechanical properties and cost-effective features. We select the oil-based ferrofluid, because it has suitable viscosity, high saturation magnetization and good stability.

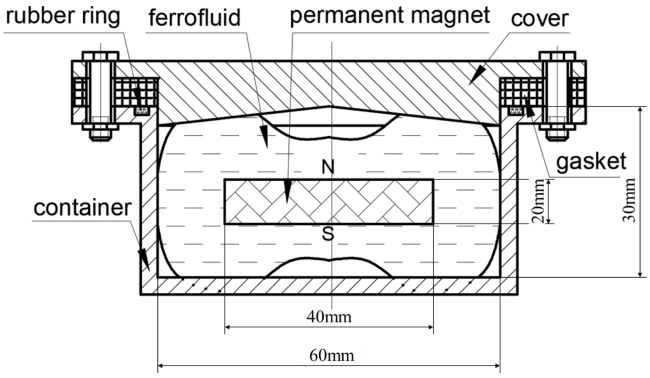

Fig. 1. Scheme of ferrofluid dynamic vibration absorber.

2.2. Energy dissipation principle and oscillating system model of ferrofluid dynamic vibration absorber

The ferrofluid dynamic vibration absorber consists of a container and a permanent magnet coated with ferrofluid. The movement of the permanent magnet covered with ferrofluid inside the container under an external oscillatory inertia force leads to a viscous dissipation of the oscillating system energy. In this paper, the damping performance is tested by the free vibration of an elastic plate with one end fixed and the other free, as shown in Fig. 3. Therefore,

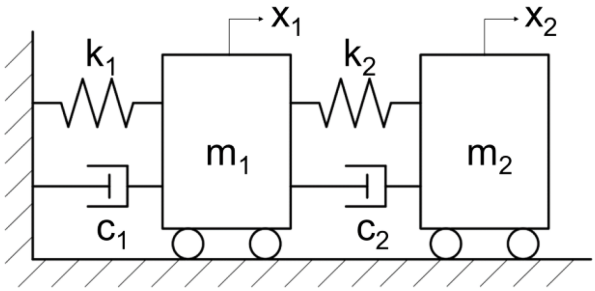

Fig. 2. The oscillation system model of two degrees of freedom.

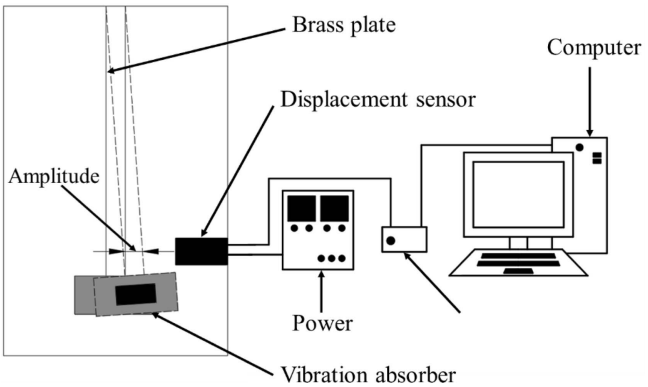

Fig. 3. Schematic diagram of experimental apparatus for the measurement of the damping performance.

the elastic plate and vibration absorber constitute a two degree of freedom damping system, which can be simplified to the model shown in Fig. 2. The dynamic differential equation of the system is as follows:

$$m_1\ddot{x}_1 + (c_1 + c_2)\dot{x}_1 + (k_1 + k_2)x_1 - c_2\dot{x}_2 - k_2x_2 = 0 \quad (1)$$

$$m_2\ddot{x}_2 - c_1\dot{x}_1 - k_2x_1 + c_2\dot{x}_2 + k_2x_2 = 0 \quad (2)$$

where m_1 is the mass of the elastic plate, container and ferrofluid, m_2 is the mass of permanent magnet, x_1 and x_2 are the displacements of the elastic plate and the permanent magnet respectively, c_1 and c_2 are damping coefficient of elastic plate and shock absorber respectively, k_1 and k_2 are stiffness coefficient of elastic plate and shock absorber respectively. k_2 is mainly affected by magnetic restoring force and c_2 is mainly affected by viscosity and shear area of ferrofluid. Thus, large number of experiments are carried out on the experimental platform under the conditions of different amplitude, cone angle of cover, mass of ferrofluid and gasket thickness. The influence of these factors on the damping performance is studied, and the performance is predicted by machine learning method.

2.3. Experiments

Figure 3 shows the experimental apparatus for the measurement of damping performance. The experimental apparatus mainly consists of bracket, brass plate, laser displacement sensor, data collector, power supply and computer. The bracket is made of non-magnetic aluminum alloy. The length of the cantilever brass plate is 1200 mm and the free vibration frequency is 1.1 Hz. In the experiment, given an initial amplitude of the free end of the brass plate (as shown in Fig. 3), the shock absorber vibrates together with the brass plate. A displacement sensor measures the displacement of brass plate in the process of vibration. The laser displacement sensor is HL-G108-S-J produced by Panasonic company in Japan. The data collector is DI-710 produced by DATAQ instruments company in American. It can store and transmit the displacement data obtained by the laser displacement sensor to the computer. Finally, the vibration displacement data is processed and analyzed by computer program.

In this paper, we use η to measure the damping performance of the ferrofluid dynamic vibration absorber. Its formula is:

$$\eta = \frac{t_1 - t_2}{t_1} \times 100\% \quad (3)$$

where t_1 is the vibration stop time (when the amplitude first attenuates to less than 0.1 mm) of cantilever brass plate with the same weight as the vibration absorber, t_2 is the vibration stop time of cantilever brass plate with vibration absorber. The greater the damping efficiency η is, the better the damping performance is.

2.4. The machine learning model

BP (backpropagation) neural network is a typical multilayer feedforward neural network, which has the ability to approximate any continuous function and nonlinear mapping. Its topology includes input layer, hidden layer and output layer. Each neuron in adjacent layer is completely connected, but the neurons in the same layer are not connected. The principle of BP neural network is to study and adjust the connection weights and thresholds of neurons according to the input and output of given samples, in order to make the network approach the mapping relationship between input and output. The training process is essentially an information positive

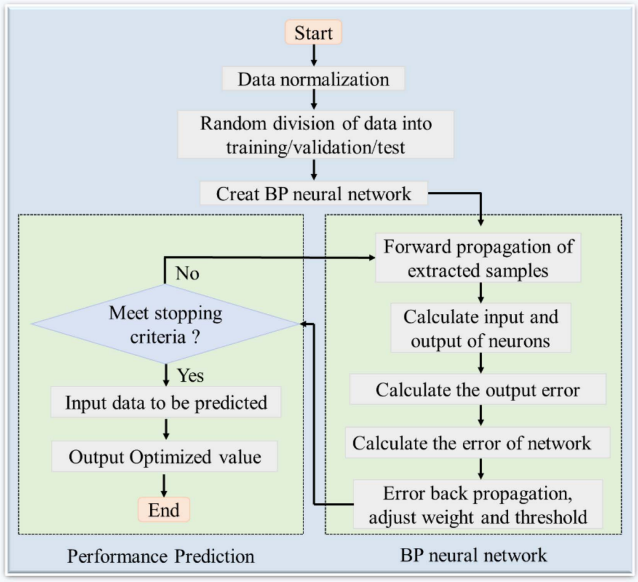

Fig. 4. (Color online) Framework of predicting damping efficiency by BP neural network.

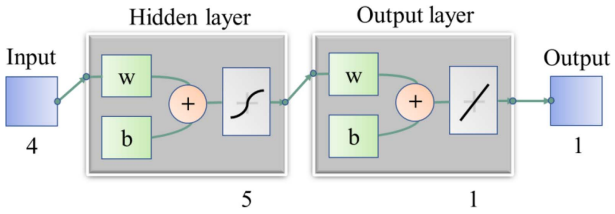

Fig. 5. (Color online) Topological structure of BP neural network model.

transmission and error back propagation [17]. The framework of BP neural network is shown in Fig. 4. BP neural network model can further deal with complex nonlinear problems, and has good fault tolerance and strong associative memory ability. In this study, the experimental data is divided into training data (70 %), validation data (15 %) and test data (15 %). We set amplitude, cone angle of cover, mass of ferrofluid and thickness of gasket as input parameters and damping efficiency as output parameter. The BP neural network structure is constructed according to the characteristics of fitting nonlinear function, as shown in Fig. 5. These algorithms are implemented on MATLAB R2020a platform. The processor adopts Intel Core i7-8550u CPU and supports 4-core 8-thread parallel computing, and its RAM is 8G.

3. Results and Discussion

3.1. Damping performance experimental results

The influence of initial amplitude, mass of ferrofluid, cone angle of cover and thickness of the gasket on the damping performance are studied by experiments. The results and analysis are as followed. The diameter and thickness of the cylindrical permanent magnet used in the experiment is 40 mm and 20 mm.

3.1.1. Influence of the mass of ferrofluid on the damping performance under different cone angles

The thickness of the gasket in this experiment is 5 mm and the initial amplitude is 1 mm. The damping efficiency curves of the ferrofluid dynamic vibration absorber are obtained with different mass of ferrofluid at the cone angle 5°, 10° and 15° of the cover, as shown in Fig. 6.

It can be seen from Fig. 6 that the damping efficiency increases first and then decreases with the increase of the mass of ferrofluid. The damping efficiency is low when the ferrofluid is insufficient, as the permanent magnet will strike the shell with little buffering ferrofluid. However, the viscous shear and energy dissipation of permanent magnet and ferrofluid is enhanced in the vibration process with the increase of the mass of ferrofluid. Thus, the

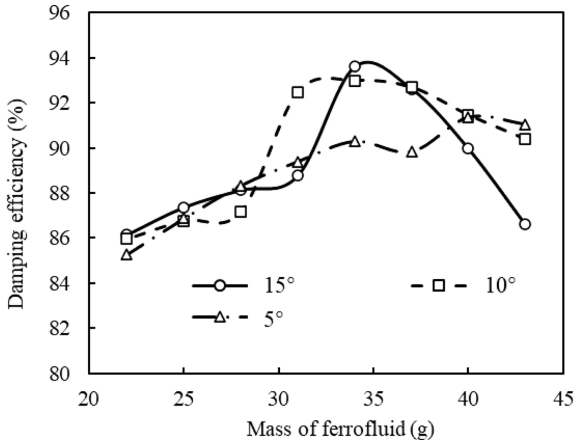

Fig. 6. The damping efficiency varies with the mass of ferrofluid at different cone angles of cover.

damping performance can be greatly improved. If we continue increase the mass of ferrofluid, the damping efficiency will be greatly reduced. The main reason is that the gap between the permanent magnet coated with ferrofluid and the shell is thinner, which will reduce the friction energy consumption between the ferrofluid and the shell. At the same time, it also hinders the movement of the permanent magnet in ferrofluid, resulting in the reduction of energy consumption.

Meanwhile, the cone angle of cover has little effect on the damping performance when the mass of ferrofluid is small. The effect of cone angle on the damping performance changes significantly when the mass of ferrofluid is more than 31 g. The main reason is that the ferrofluid possesses different velocity gradient under different cone angle in the vibration process. The larger the cone angle, the greater the velocity gradient provided by the end cover. If the mass of the ferrofluid continues to increase, the larger cone angle of the cover will hinder the flow of the ferrofluid, which will reduce the damping efficiency. Thus, the value of the cone angle will affect the damping efficiency of the vibration absorber.

3.1.2. Influence of the initial amplitude value on the damping performance under different cone angles

In the experiment, the thickness of the gasket is 5 mm and the mass of the ferrofluid is 34 g. The damping efficiency of the ferrofluid dynamic vibration absorber with different initial amplitudes of 1 mm, 2 mm, 3 mm, 4 mm and 5 mm is obtained under different cone angles of cover, as shown in Fig. 7.

The value of the initial amplitude has little effect on the damping efficiency, as shown in Fig. 8. The vibration absorber has obvious damping performance under different

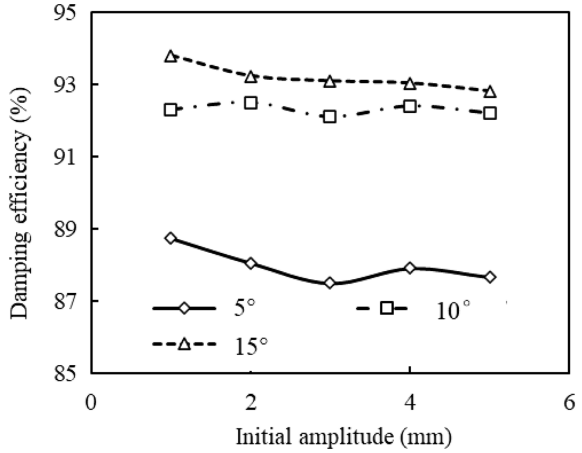

Fig. 7. The damping efficiency varies with the initial amplitude at different cone angles of cover.

values of initial amplitude. There is a big difference in damping efficiency under different cone angles of cover. The damping efficiency of the vibration absorber is the highest when the cone angle of the cover is 15° at these above initial amplitude. It's due to the fact that the larger the cone angle of the cover is, the greater the velocity gradient of the ferrofluid is. Thus, the viscous energy dissipation of the vibration absorber is increased. That agrees with our previous result.

3.1.3. Influence of the thickness of gasket on the damping performance under different mass of ferrofluid

In the experiment, the cover with a cone angle of 15° is used. We get the influence of the gasket thickness on the damping efficiency under different mass of ferrofluid, as shown in Fig. 8.

It can be seen from the Fig. 8 that the damping efficiency of the ferrofluid dynamic vibration absorber first increases and then decreases with the increase of gasket thickness. The reason for this is that the cover hinders the movement of the permanent magnet covered with ferrofluid when the thickness of gasket is small and the cover couldn't provide restoring force for permanent magnet when the thickness of gasket is large. All of this can lead to the decrease of damping efficiency. Moreover, the thickness of gasket is different to achieve the best damping performance under different mass of ferrofluid. The thickness of the gasket to achieve the best damping performance is increased with the increase of the mass of ferrofluid. This is consistent with our previous analysis. The vibration efficiency η reaches 93.88 % when the height of the gasket is 6 mm, the mass of ferrofluid is 40 g, the cone angle of cover is 15° and the initial amplitude is 1mm.

3.2. Prediction of damping performance by machine learning

The criteria for evaluating the prediction performance of BP neural network are mean squared error (MSE) and determination coefficient (R^2). The MSE is zero and R^2 is one in the ideal model. Formula (4) and (5) show the expressions used to calculate MSE and R^2, respectively.

$$MSE = \frac{1}{N}\Sigma_{I=1}^{N}(y_i^{actual} - y_i^{predicted})^2 \tag{4}$$

$$R^2 = 1 - \frac{\Sigma_{i=1}^{N}(y_i^{actual} - y_i^{predicted})^2}{\Sigma_{i=1}^{N}(y_i^{actual} - \overline{y^{actual}})^2} \tag{5}$$

where N is the number of data, y^{actual} is the ith actual data, $y^{predicted}$ is the ith predicted data of the neural network and $\overline{y^{actual}}$ stands for the average of the measured real value.

Next, the prediction performance of BP neural network is introduced and discussed. The training time and

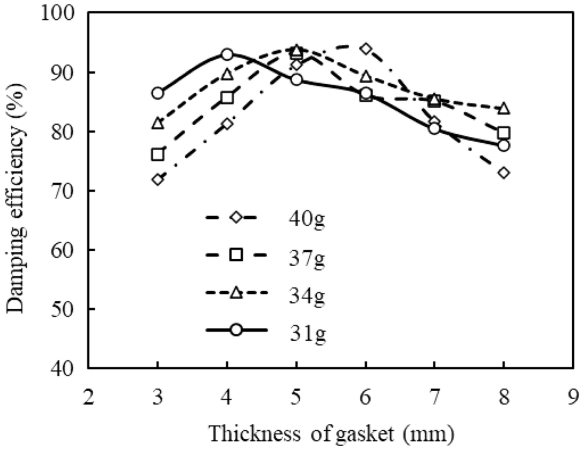

Fig. 8. The damping efficiency varies with the thickness of gasket at different cone angles of cover.

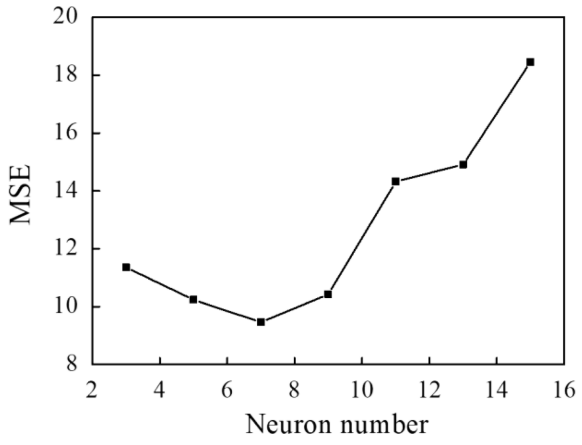

Fig. 9. Prediction performance of BP neural network with different number of hidden layer neurons.

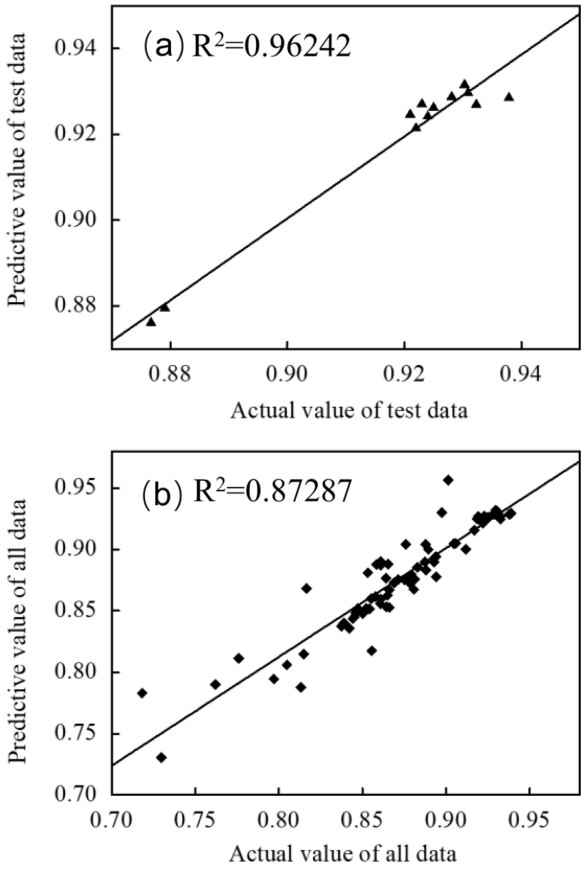

Fig. 10. Regression performance of BP neural network with 7 hidden layer neurons (a) test data (b) all data.

accuracy of BP neural network varies with the number of hidden layer neurons. Thus, the influence of the hidden layer neurons number on the prediction performance of damping efficiency is analyzed. According to the empirical formula, the range of neuron number is from 3 to 15. We calculate MSE under different neuron numbers (each data is calculated 100 times and the average value is taken). The prediction accuracy changes with the number of neurons, as shown in Fig. 9. The prediction performance is the best when the number of hidden layer neurons is 7. In this case, the MSE of test data is 8.90704.

Then, the linear regression performance of BP neural network is studied when the number of hidden layer neurons is 7, as shown in Fig. 10. The determination coefficient R^2 of test data is 0.96242 and all data is 0.87287. The closer to 1 the correlation coefficient is, the better the performance of the model is. Fig. 11 indicates that the predictive errors are mainly distributed within ± 0.4 %. The hit rate of the model is 91.67 % when the predictive errors are within ± 0.8 % and the hit rate of the model is 75 % when the predictive errors are within ± 0.4 %. These results indicate that BP neural network can

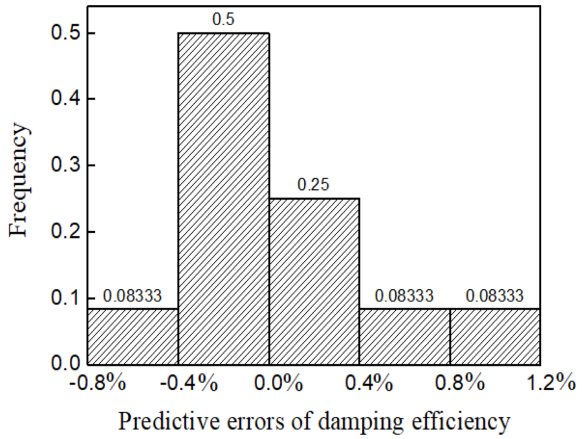

Fig. 11. Frequency distribution of predictive errors for BP neural network model.

Table 1. The range and the incremental step of the four influence factors.

Influence factor	The range of value	Incremental step size
The mass of ferrofluid	22-40 g	0.1
Initial amplitude	1-5 mm	0.1
The cone angle of cover	5-15°	5
The thickness of gasket	1-8 mm	1

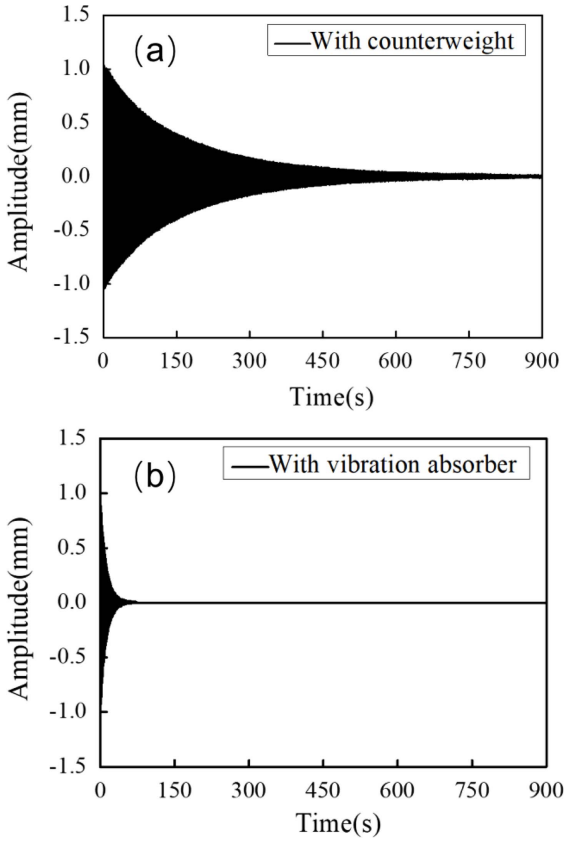

Fig. 12. Vibration curves of brass plate (a) with ferrofluid dynamic vibration absorber (b) with counterweight.

accurately estimate the damping efficiency.

According to the established neural network model, the optimal value of the influence factors is found by search algorithm. The range and the incremental step of the four influence factors are shown in Table 1. The parameters of our experiments are also in this. The best damping efficiency is predicted to be 94.03 % when the initial amplitude is 1mm, the mass of ferrofluid is 36.9 g, the cone angle of cover is 15° and the thickness of gasket is 5.2 mm. To confirm this, the damping efficiency of the ferrofluid shock absorber is obtained by experiments at above-mentioned value. The amplitude during vibration process is shown in Fig. 12. The damping efficiency is 94.08 %, which is close to the predictive value. This indicates that machine learning is significant to design the ferrofluid dynamic vibration absorber. In this research, the BP neural network is trained according to a designated structure. In this case, whether the optimal values of the four influence factors are applicable to other absorbers still need further study. However, we believe that through training the BP network using the data of absorbers with different size, the BP network could predict the optimal value of absorbers with various sizes.

4. Conclusion

We design a ferrofluid dynamic vibration absorber based on the second buoyancy principle of ferrofluid, which possesses advantages of simple structure, long life time and zero energy consumption. The energy of the vibration absorber is dissipated mainly by friction and elastic deformation of ferrofluid adsorbed by permanent magnet. The effects of the initial amplitude, the mass of the ferrofluid, the thickness of the gasket and the cone angle of the cover on the damping performance are studied on the experimental apparatus. The results show that the initial amplitude has little influence on the damping efficiency; the damping efficiency increases first and then decreases with the increase of the mass of ferrofluid and the gasket thickness; the appropriate cone angle of the gasket can improve the damping efficiency of the shock absorber. Based on the experimental data, a model which could well predict the damping efficiency is established by BP neural network. According to the model, we use search algorithm to find the optimal value of each influence factor and obtain the best damping efficiency as high as 94.03 %, which is close to the experimental value under the same parameters. Our work provides an innovative method for accurately predicting the damping efficiency of vibration absorber, which shedding light into the rapid design of high efficiency vibration absorber.

Acknowledgement

This work is supported by National Natural Science Foundation of China [grant number 51735006, 51927810, U1837206].

References

[1] D. F. Ledezma-Ramírez, P. E. Tapia-González, N. Ferguson, M. Brennan, and B. Tang, Applied Mechanics Reviews **71**, 060802 (2019).
[2] R. E. Rosensweig, Annual Review of Fluid Mechanics 437 (1987).
[3] C. Rinaldi, A. Chaves, S. Elborai, X. T. He, and M. Zahn, Current Opinion in Colloid & Interface Science **10**, 141 (2005).
[4] E. Jarkova, H. Pleiner, H. W. Müller, A. Fink, and H. R. Brand, The European Physical Journal E **5**, 583 (2001).
[5] X. Liu, A. Song, S. Chen, Q. Li, R. Sun, J. Yang, and D. Li, Materials Letters **252**, 110 (2019).
[6] Z. Wang, G. Bossis, O. Volkova, V. Bashtovoi, and M. Krakov, Journal of Intelligent Material Systems and Structures **14**, 93 (2003).
[7] J. Yao, J. Chang, D. Li, and X. Yang, Journal of Magnetism and Magnetic Materials **402**, 28 (2016).
[8] J. Yao, D. Li, X. Chen, C. Huang, and D. Xu, Journal of Fluids and Structures **90**, 190 (2019).
[9] W. Yang, P. Wang, R. Hao, and B. Ma, Journal of Magnetism and Magnetic Materials **426**, 334 (2017).
[10] C. Huang, J. Yao, T. Zhang, Y. Chen, H. Jiang, and D. Li, Journal of Magnetics **22**, 109 (2017).
[11] A. Missiles, Space and Electronics Group 1 (1967).
[12] R. E. Rosensweig, Nature **210**, 613 (1966).
[13] M. I. Shliomis, Journal of Experimental and Theoretical Physics **34**, 1291 (1972).
[14] S. Sudo and A. Nakagawa, International Journal of Modern Physics B **19**, 1520 (2005).
[15] W. Yang, D. Li, and Z. Feng, Journal of Vibration and Control **19**, 183 (2012).
[16] J. Yao, J. Chang, D. Li, and X. Yang, Journal of Magnetism and Magnetic Materials **402**, 28 (2016).
[17] Hagan, T. Martin, Demuth, B. Howard, Beale, and H. Mark, Neural network design, China Machine Press, Beijing (2002).